14 Friedreich's Ataxia and More: Optical Coherence Tomography Findings in Rare Neurological Syndromes

Chiara La Morgia and Michele Carbonelli

14.1 Friedreich's Ataxia

Friedreich's ataxia (FA) is an autosomal recessive slowly progressive neurodegenerative disorder starting usually in young adulthood or childhood [1]. FA is characterized by spinocerebellar and sensory ataxia with absence of deep tendon reflexes, dysarthria, hypertrophic cardiomyopathy and scoliosis [2]. FA is due to a GAA triplet expansion in the first intron of the frataxin gene (FXN) on chromosome 9q13-q21.1. A minority of FRDA patients are compound heterozygotes for the GAA triplet expansion and a point mutation [3].

Frataxin is a mitochondrial protein with a crucial role in the insertion of Fe-S cluster in different enzymes of the mitochondrial respiratory chain and in particular complex I, II and III and aconitase [4, 5]. The abnormal function of FXN leads to dysregulation of cellular iron metabolism with mitochondrial accumulation [6]. Evidence of mitochondrial defective respiration has been demonstrated in the heart and muscle of FA patients [7, 8]. Recent studies demonstrated that mitochondrial dysfunction induced by frataxin is also related to abnormal calcium handling in the mitochondria leading to increased autophagy [9]. Overall, frataxin deficiency leads to abnormal iron homeostasis [10] and increased oxidative stress [11, 12].

C. La Morgia (✉)
UOC Clinica Neurologica, IRCCS Istituto delle Scienze Neurologiche di Bologna, Bologna, Italy

Dipartimento di Scienze Biomediche e Neuromotorie, Università di Bologna, Bologna, Italy
e-mail: chiara.lamorgia@unibo.it

M. Carbonelli
UOC Clinica Neurologica, IRCCS Istituto delle Scienze Neurologiche di Bologna, Bologna, Italy

A. Grzybowski, P. Barboni (eds.), *OCT and Imaging in Central Nervous System Diseases*, https://doi.org/10.1007/978-3-030-26269-3_14

Visual system involvement is well characterized in FA [13]. In particular, abnormalities of the visual efferent system such as fixation instability (square wave jerks), saccadic dysmetria, disrupted pursuit, and vestibular abnormalities have been reported [13]. Moreover, optic neuropathy, optic radiation abnormalities and retinitis pigmentosa have been described in FA patients [14–19].

The optic neuropathy described in FA is usually asymptomatic and does not affect central vision [16]. The most severe visual phenotype has been associated with large GAA expansion of the FTX gene and with compound heterozygous mutations [16]. Visual evoked potentials demonstrated delayed latency and reduced amplitude of the cortical responses [15, 16]. Visual field defects may vary from small paracentral or arcuate to diffuse and generalized defects [16]. Only rarely FA patients present an acute loss of visual acuity, which resembles Leber's hereditary optic neuropathy (LHON) [16].

A few optical coherence tomography (OCT) studies are available for FA. These described a diffuse reduction of the retinal nerve fiber layer (RNFL) thickness without a preferential involvement of the temporal quadrant [16–19], unlike mitochondrial optic neuropathies [20]. The severity of optic atrophy can be variable and usually is not associated with a subjective visual complaint [15, 16]. Specifically, time-domain OCT studies reported a generalized RNFL thinning in FA patients [16–18]. Interestingly, in the largest OCT series (63 FA patients) available to now, the only sector with a significant RNFL thinning was the superior [18] (Table 14.1).

Retinal nerve fiber layer thinning significantly correlated with age at onset and International Cooperative Ataxia Rating Scale (ICARS) in the series (n = 26) by Fortuna and coauthors [16]; with ICARS score, disease duration, visual acuity (VA) and low-contrast letter VA in the series (n = 23) by Noval and coauthors [17] and with VA, GAA repeat length, Friedreich's Ataxia Rating Scale (FARS) and age at onset in the series (n = 63) by Seyer and coauthors [18] (Table 14.1).

The only spectral domain (SD) OCT study available to date documented a reduction of the average RNFL thickness and in all four optic disc sectors in 10 FA patients [19]. Moreover, ganglion cell thickness was significantly reduced in superior and inferior macula [19] (Table 14.1).

Macular thickness has been reported as normal in one study [17], significantly reduced [19] and below the 1st percentile of controls in 20.7% of the FA patients examined in another series [18] (Table 14.1).

Correlation of OCT measurement with VA is not consistent across the studies and the degree of VA loss is reported as variable, but usually not clinically significant [16, 17]. Differently, low contrast visual acuity is significantly reduced in FA

Table 14.1 OCT findings in Friedreich's ataxia

	OCT	N. of pts	Main findings	Correlations
Fortuna et al. [16]	TD-Stratus	26	↓ avg RNFL ↓ RNFL in all 4 sectors	ICARS, age at onset
Noval et a. [17]	TD-Stratus	17	↓ avg RNFL in 75% Temporal RNFL thickness normal Normal Macular morphology and thickness	ICARS, disease duration, VA, low-contrast VA
Seyer et al. [18]	TD-Stratus	63	↓ RNFL (52.7% of eyes below 5th percentile of controls) Only superior thickness significantly lower	VA, GAA expansion, age at onset, FARS
Seyer et al. [18]	SD-Cirrus	23	Macular thickness below the 1st percentile of controls in 20.7%	Not significant
Dağ et al. [19]	SD	10	↓ avg RNFL ↓ RNFL in all 4 quadrants ↓ Peripapillary and foveal retinal thickness Choroidal thickness not significant ↓ GC thickness in superior and inferior macula	VA, ICARS (RNFL thickness) Disease duration (foveal thickness)

RNFL retinal nerve fiber layer, *avg* average, *ICARS* International Cooperative Ataxia Rating Scale, *FARS* Friedreich's Ataxia Rating Scale, *VA* visual acuity

patients [17]. Fundus oculi abnormalities are detected only in a small percentage of the FA subjects with loss of retinal nerve fibers documented by OCT [17].

Overall, OCT measurements in FA are able to detect subclinical optic neuropathy in the large majority of FA cases (about 70%) being a more sensible measure of optic nerve degeneration than other metrics (visual acuity, visual fields and/or fundus examination). It is not clear yet why the papillomacular bundle is not primarily affected in FA, even if a mitochondrial dysfunction is well known in FA.

In line with OCT data, visual evoked potentials (VEPs) documented an increased P100 latency and reduced amplitude of cortical responses [15, 16] in the large majority of patients. These electrophysiological and anatomical data suggest a slowly progressive degeneration of the anterior and posterior optic pathway, as proved also by the increased diffusion in optic radiations demonstrated in FA patients by magnetic resonance imaging studies [16].

Examples of swept-source OCT images and fundus oculi pictures are provided for two FA patients presenting, respectively a mild and severe optic atrophy (Fig. 14.1).

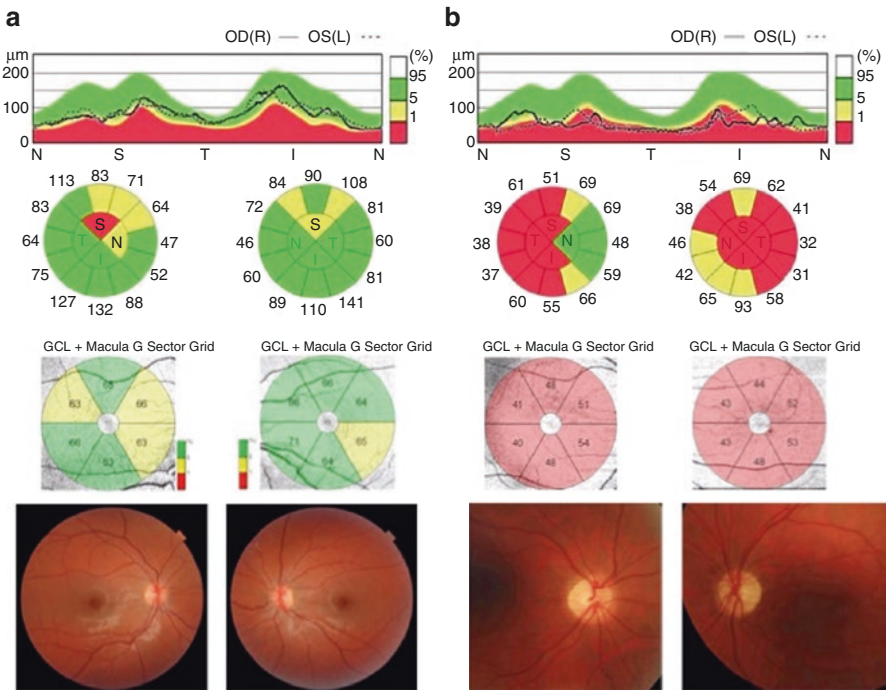

Fig. 14.1 (Friedreich) (**a**) This is a 20 year-old female who suffered ataxic gait since she was 15 years. She does not complain specific visual disturbances. Her visual acuity is 12/10 bilaterally and visual fields showed a small nasal step in the RE and a small superior defect in the LE. OCT shows a mild superior RNFL thinning and a small GCC defect. Fundus oculi showed mild temporal pallor bilaterally. (**b**) This is a 43 year-old female who presented gait ataxia since she was 13 years old. She started complaining visual loss since she was 38 years and her visual acuity progressively worsened over time. Her visual acuity is now 1.6/10 in the RE and 0.5/10 in the LE. Visual fields showed generalized defect with relative central sparing bilaterally. OCT shows generalized RNFL thinning with relative nasal sparing and diffuse GCC loss. Fundus oculi showed diffuse pallor more evident on the temporal sector

14.2 Jansky-Bielschowsky Disease (CLN2)

Jansky-Bielschowsky disease (JBD) is a late infantile neuronal ceroid lipofuscinosis (LINCL) disorder due to mutation of the *CLN2* gene (cr 11p15), which encodes for the tripetidylpeptidase 1 protein [21, 22]. Similarly to other Neuronal Ceroid Lipofuscinosis (NCL) JBD is a lysosomal storage disease characterized by the accumulation of autofluorescent material in the cytoplasm of neurons [23]. JBD disease is characterized by mental and motor retardation, psychomotor regression, ataxia, seizures and visual dysfunction [23].

Visual dysfunction is common in NCL and usually manifests early in juvenile forms and later in the LINCL [24]. The typical ocular manifestation of NCL is retinal degeneration of variable severity (from mild pigmentary changes to Bull's eye maculopathy

to severe outer retina atrophy) [24]. Retinal changes in LINCL have been documented by fundus oculi examination, histopathology and electrophysiological studies [24–27]. Furthermore, the presence of inner retina and optic nerve degeneration has been demonstrated in different animal models of NCL [28–31]. Besides outer retina degeneration, optic atrophy is a frequent finding in LINCL [25, 32]. The only OCT study available to now in JBD applied a comprehensive ophthalmologic evaluation in 25 LINCL patients with mutations in the *CLN2* gene [33]. The protocol included fundus oculi, spectral domain macula OCT, fluorangiography (FA) and indocyanine green angiography (IGA) and was carried out under anesthesia. The results obtained were used to generate a Weill Cornell LINCL Ophthalmologic Severity Scale score. According to the degree of pigmentary changes at fundus oculi examination, FA and IGA and the severity of outer retina degeneration documented by OCT the patients were graded as score 0–5 (from normal to severe changes). The average score in this case series was 2.6. This score correlated strongly with the neurological score suggesting that the retinal involvement is parallel to the neurological deterioration. Interestingly, the authors failed to document any abnormality in the anterior segment, at difference with other lysosomal storage diseases. The posterior segment showed variable degrees of optic nerve and retinal atrophy. In particular, retinal degeneration typically starts from the fovea in which the first pigmentary changes are visible expanding to the far periphery [33]. The OCT was able, in this case series, to detect subtle abnormalities not visible at fundus examination or with FA. The OCT changes documented by Orlin and coauthors for the 5 stages were: *Stage 1*: normal; *Stage 2*: Normal retinal layers immediately adjacent at fovea; immediately outside fovea, outer retinal/photoreceptor atrophy; *Stage 3*: Outer retinal atrophy/photoreceptor loss extending to 1.0 disc diameter from fovea; retinal layers appear normal outside fovea; *Stage 4*: Early buildup of outer retinal hyper-reflective material in macula; more extensive outer retinal abnormalities extending 1.0–2.0 disc diameters from fovea; beyond 2.0 disc diameters, outer retina appears normal; *Stage 5*: Severe retinal thinning with generalized loss of photoreceptors and outer retina, involving the entire macula; extensive clumps of outer retinal hyper-reflective material; thickness map shows central thinning with paracentral thickening, with outer ring of further thinning (with bull's eye appearance); outer retinal changes also found outside the macula [33]. The majority of patients in this case series presented normal or mildly abnormal ocular findings (32% stage 0, 24% stage 1, 8% stage 3, 24% stage 4 and 12% stage 5) [33].

14.3 Juvenile Neuronal Ceroid Lipofuscinosis-Batten Disease (CLN3)

Juvenile neuronal ceroid lipofuscinosis (JNCL) is the most frequent form of the NCL disorders due to biallelic mutations in the *CLN3* gene [34]. Visual loss is usually the earliest symptom of the disease manifesting between 4 and 8 years of age. The ophthalmological features of CLN3 patients include optic nerve pallor, bull's-eye maculopathy, and intraretinal pigmentation, associated with abnormalities at electrophysiological testing. Neurological features include mental retardation, extrapyramidal symptoms and seizures.

Ku and coauthors extensively investigated the clinical phenotype of retinal degeneration in CLN3 patients [35]. In this case series OCT demonstrated in patients with preserved visual acuity and late-onset disease a focal preservation of the ellipsoid zone and outer nuclear layer in the fovea, despite the presence of macular edema. At difference, in patients with decreased visual acuity and early-onset disease, a moderate-severe foveal outer nuclear layer and ellipsoid zone loss were evident, in association in some patients with hyperreflective deposits at the level of the retinal pigment epithelium. Electroretinography showed a rod-cone pattern of dysfunction in 6 patients and were completely undetectable in 2 patients [35]. Ophthalmoscopic findings included macular edema, mild intraretinal bone spicule migration, and significant macular atrophy. Fundus autofluorescence imaging showed central retinal hypoautofluorescence.

In CLN2 the opthalmological findings include a complete retinal atrophy starting from bull's eye maculopathy and optic nerve pallor. OCT show a centripetal degeneration of the outer layers starting from the parafoveal region in the ellipsoid zone and developing into the fovea and outward to the periphery. In CLN3 patients with relatively short disease duration, Preising and coauthors [36] described by SD-OCT a general reduction of the entire retinal thickness resulting mostly from photoreceptor-associated and the inner nuclear layers (first and second neurons). At difference, the retinal nerve fiber layer (RNFL) and the ganglion cell layer (GCL+) were described as within normal thickness values, even though the presence of gliosis and irregular inner limiting membrane (ILM) suggest a degeneration of retinal ganglion cells (RGCs) constituting the optic nerve. The retinal pigmented epithelium (RPE) layer thickness is described as within normal values. This pattern is different from macular dystrophies like ABCA4-associated cone-rode dystrophy (CRD) where the first neuron layer is affected before the second neuron layer and the third neuron is preserved. The preservation of the first neuron outside the macula suggests in the youngest CLN3 case a centrifugal progression of the retinal degeneration, which corresponds to the later stages of CLN2 retinal degeneration. In the later stages of the disease, also the optic nerve is affected showing neuronal loss [37].

14.4 DNMT1 Disease

DNA (cytosine-5)-methyltransferase 1 (DNMT1) disease is a complex neurodegenerative disorder due to autosomal dominant mutations in the *DNMT1* gene (DNA-methyltransferase 1) [38].

Two distinct phenotypes have been described in association with mutations in the *DNMT1* gene: the autosomal dominant cerebellar ataxia, deafness and narcolepsy (ADCA-DN) [39] associated with mutations in exon 21 of the *DNMT1* gene and the hereditary sensory autonomic neuropathy with dementia and hearing loss type IE (HSAN IE), described in association with mutations in exon 20 [38]. Recently, our group demonstrated that the boundaries between these two distinct entities are less pronounced [40]. In fact, both diseases share the presence of narcolepsy as a prominent feature [40]. Moreover, we demonstrated that subclinical optic atrophy is a common finding to both phenotypes [40].

Visual acuity was normal in all five DNMT1 patients included in the study (two with the ADCA-DN and three with the HSAN IE phenotype). Fundus oculi disclosed temporal pallor in one ADCA-DN case, diffuse pallor in the other ADCA-DN and mild temporal pallor of the optic disc in all three HSAN IE subjects. Pattern VEPs were abnormal in both ADCA-DN probands, showing increased latency and decreased amplitude of cortical responses, whereas they were normal in HSAN IE patients [40]. OCT showed reduction of the RNFL thickness more evident in the temporal than in the superior and inferior quadrants with nasal sparing in one ADCA-DN patient, more diffuse in the other ADCA-DN patient with nasal sparing. In the HSAN IE cases OCT disclosed a diffuse reduction of retinal nerve fiber layer thickness in one case, a diffuse reduction with nasal sparing in the second case, and temporal and less evident superior/inferior quadrants thinning in the third case.

Macular ganglion cell layer (GCL) analysis disclosed diffuse atrophy in both ADCA-DN probands and diffuse thinning in all three HSAN IE subjects [40].

Examples of swept-source OCT (RNFL and macular GCL) and fundus oculi images are reported for two DNMT1 patients carrying respectively the p.Glu575Lys mutation at exon 21 and the p.Pro507Arg mutation at exon 20 [40] (Fig. 14.2).

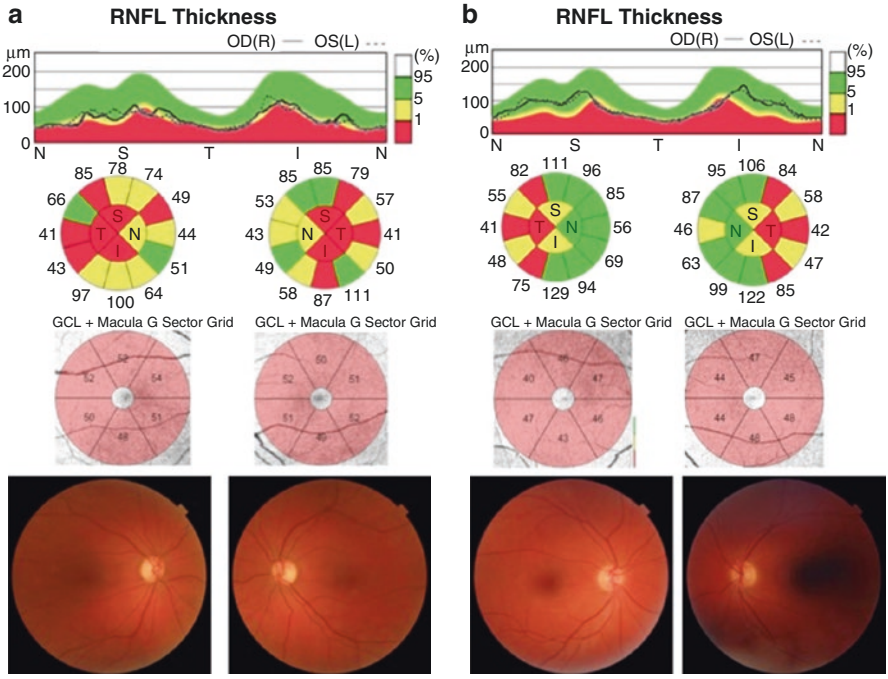

Fig. 14.2 DNMT1. (**a**) This is a 49-year old female carrying the p.Glu575Lys mutation at exon 21 in the DNMT1 gene. Visual acuity is 10/10 bilaterally. OCT shows a diffuse optic nerve fiber thinning, as demonstrated also by the diffuse GCC defect. Fundus oculi image show increased optic disc excavation and mild temporal pallor. (**b**) This is a 38-year old male carrying the p. pro-507Arg mutation at exon 20. Visual acuity is 12/10 bilaterally. OCT shows temporal RNFL thinning, as well as fundus oculi reveals a mild temporal pallor

Interestingly, optic atrophy was previously reported in the ADCA-DN phenotype [41, 42] but never described in the HSAN IE phenotype. OCT investigation in our DNMT1 case series revealed a subclinical optic nerve involvement in all cases with a prevalent involvement of the temporal sector and relative nasal sparing that resembles the pattern observed in mitochondrial optic neuropathies [20]. The mitochondrial pattern of optic nerve degeneration may be explained by the possible effect of defective methylation of nuclear DNA on nuclear encoded mitochondrial proteins [43] or a direct effect on DNA methylation of the mitochondrial-targeted isoform of DNMT1 [44, 45]. At this regard, interestingly DNMTs including DNMT1, through epigenetic regulation, may play a role in the development and homeostasis of photoreceptors and other retinal neurons within the mammalian retina [46].

14.5 Hereditary Spastic Paraplegia Due to SPG7 Mutations

Hereditary spastic paraplegias (HSP) are a heterogeneous group of neurodegenerative disorders characterized by a variable phenotypic expression, which includes a pure spastic paraparesis or "uncomplicated" and a "complicated" form. The genetic basis of HSP is heterogeneous including autosomal dominant, autosomal recessive, X-linked, or maternally inherited (mitochondrial) inheritance [47].

More than 56 HSP loci and 41HSP-related genes have been identified [47].

Mutations in the *SPG7* gene are responsible for autosomal recessive SPG7-HSP. The first *SPG7* mutation was identified in 1998 [48, 49]. *SPG7* gene encodes for paraplegin, which is a metalloprotease protein belonging to the AAA (ATPase associated with various cellular activities) proteins. Paraplegin is a mitochondrial protein localized to the inner mitochondrial membrane and it assembles with the paralogous AFG3L2 protein in the mAAA protease complex [50–53]. Mitochondrial dysfunction has been described in SPG7 pedigrees including OXPHOS defects in muscle biopsy [48]. Interestingly, mAAA protease like paraplegin plays also a role in the processing of the OPA1 protein [54]. Given the mitochondrial pathogenesis of SPG7 HSP, the presence of optic atrophy is expected, but not systematically investigated. Optic atrophy has been reported in the first identified pedigrees [48, 49, 53]. Klebe and coauthors extensively described the phenotype of 23 SPG7 families [55]. In a subgroup (n = 10) investigated by OCT, RNFL thinning was detected in 100% of cases even if it was symptomatic only in one case, associated with reduced visual acuity in 40% and with optic disc pallor at fundus examination in 50% of cases. These data suggest that the OCT investigation may detect subtle abnormalities in SPG7 patients and the presence of optic atrophy in the context of an

autosomal recessive spastic paraplegia should point to the *SPG7* gene. In this case series one French pedigree positive for the *SPG7* mutation presented with an isolated autosomal dominant early onset (first decade of life) progressive optic atrophy. Electroneurography disclosed in this pedigree also the presence of mixed peripheral polyneuropathy [55].

On the basis of the clinical findings of this cohort the authors proposed that *SPG7* gene should be screened in autosomal recessive or sporadic HSP patients with middle-age onset particularly if spastic paraplegia is associated with cerebellar atrophy/signs and/or optic neuropathy (also if detected only with OCT).

Van Gassen and coauthors, in another large SPG7 Dutch case-series (n = 49), demonstrated the presence of a severe optic atrophy with childhood onset in two siblings carrying a homozygous missense mutation (p.Arg470Gln, exon 10) *SPG7* mutation and in one case with compound heterozygous (p.Arg485_Glu487 and p.Leu706fs) *SPG7* mutation. For one of the p.Arg470Gln mutation carriers, postmortem tissues including the optic nerve were available. In this case a severe optic atrophy was documented. Interestingly, the p.Arg470Gln mutation was located in the ATPase AAA core domain and the authors hypothesized that the severe optic nerve involvement can be explained by a possible deleterious interaction of SPG7 with OPA1. Unfortunately, for these patients OCT data were not available [56].

Moreover, Marcotulli and coauthors have recently described a 43-year-old male SPG7 case presenting with severe congenital optic atrophy. This patient developed spastic paraparesis at 30 years of age. OCT documented reduced RNFL and macular thickness [57].

Overall, these data suggest that optic neuropathy is a common finding in SPG7-related HSP and the use of OCT screening in large cohort of HSP patients might be a useful tool to reveal subclinical optic atrophy and guide the diagnostic process.

Interestingly, Wiethoff and coauthors conducted an OCT study on 28 HSP patients including "pure" (n = 22) and "complicated" (n = 6) HSP demonstrating a significant reduction of the RNFL only in the "complicated" group. The case series included also 3 SPG7 cases and two of them, presenting a complicated phenotype, manifested a global RNFL thickness reduction, especially in the temporal quadrant [58].

We recently had the opportunity to diagnose the presence of compound heterozygous SPG7 mutations in a 24 year-old female who presented ophthalmological features (Fig. 14.3) indistinguishable from OPA1 patients. Neurological examination was unremarkable except for the presence of optic nerve temporal pallor and specifically did not reveal any sign of spastic paraparesis. This case highlights the possibility that SPG7 mutations might be associated to pure optic atrophy cases.

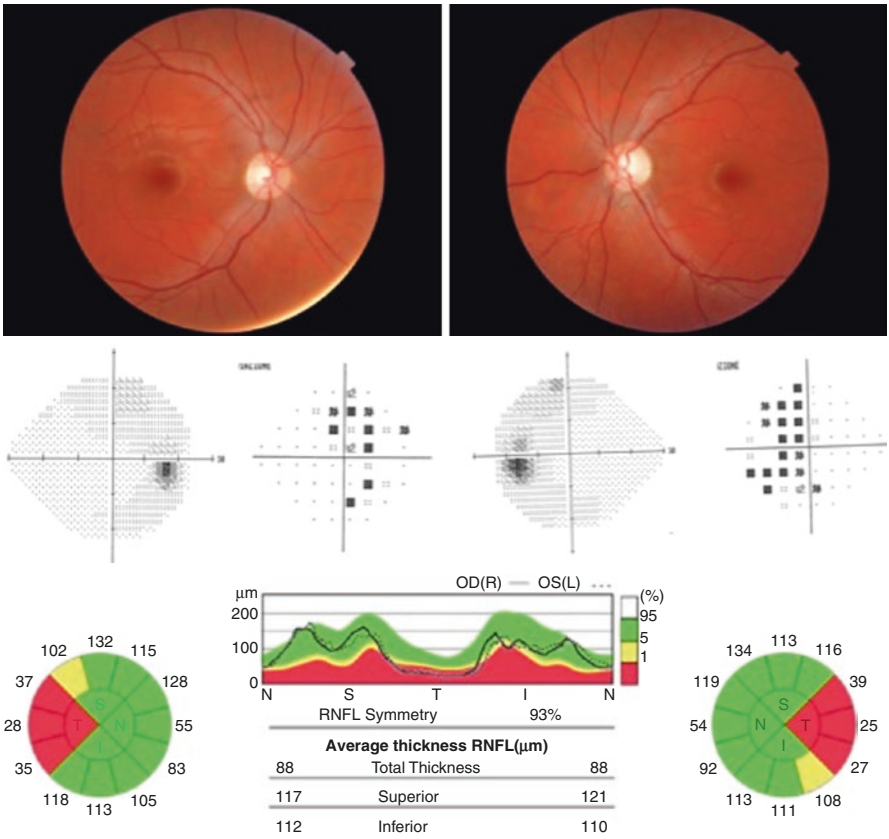

Fig. 14.3 SPG7. 24 year female carrying compund heterozygous mutations- c.524T>C (p.LI75P) + c1968_69 ins A (p.165NfsX22) in the SPG7 gene. Visual acuity is 20/32 (0.63). Fundus oculi reveals bilateral temporal optic nerve pallor. Visual fields showed small central scotoma bilaterally and OCT demonstrated temporal RNFL thinning bilaterally. Brain MRI, somatosensory and motor evoked potentials were normal. Neurological examination did not show the presence of spastic paraparesis

14.6 CADASIL

Cerebral autosomal dominant arteriopathy with subcortical infarcts and leukoencephalopathy (CADASIL) is an autosomal dominant disorder characterized by the occurrence of juvenile subcortical ischemic events, migraine, epilepsy, psychiatric disturbances and cognitive impairment in variable combinations [59]. Brain MRI typically shows T2 hyperintensity involving the white matter of the temporal pole and/or the external capsulae, but the severity of white matter involvement can be highly variable evolving into most cases to a diffuse bilateral subcortical leukoencephalopathy [60].

CADASIL is due to mutations of the *NOTCH3 (Neurogenic locus notch homolog protein 3)* gene, located on chromosome 19 [61]. Notch3 is a protein mainly expressed in vascular smooth cells with a crucial role in the control of vascular tone [62]. Cerebral vasculopathy is the main hallmark of the disease, due to the degeneration of the vascular smooth muscle cells with deposition of granular osmiophilic material, but also retinal vascular changes have been described in CADASIL [63–65]. These changes include retinal arteriolar narrowing, arteriovenous nicking and arteriolar sheating [64, 66]. Moreover, electrophysiological [67], histological [68] and OCT studies [66, 69, 70] documented a specific neurodegeneration of the neuroretina in CADASIL. In particular, Parisi and coauthors demonstrated by time-domain OCT a diffuse reduction of the RNFL thickness involving all the quadrants in 6 CADASIL patients (three asymptomatic mutation carriers) [69]. The authors interpreted these findings as secondary to the chronic vascular changes characterizing the disease. Similarly, Rufa and coauthors demonstrated with time-domain OCT a diffuse RNFL thinning in all optic nerve quadrants except the nasal one in 17 CADASIL patients. In particular, this thinning was more evident in the superior sector [70]. Fundus oculi examination revealed neuroretinal rim pallor in 41% and a crowded optic disc in 18% of the 34 CADASIL patients described by Pretegiani and coauthors [66]. The optic nerve involvement in CADASIL is also confirmed by histological findings in a postmortem study, which demonstrated diffuse demyelination in the optic nerve and chiasm with loss of nerve fibers [68]. The loss of fibers in the optic nerve is usually not associated with a reduction of the visual acuity and can be associated with variable visual field defects [66].

OCT studies are also particularly relevant for highlighting the vascular component of retinal changes in CADASIL patients. In particular, OCT-angiography studies demonstrated reduced vessel density in the deep retinal plexus (DRP) of CADASIL patients [71]. These abnormalities may reflect pericyte dysfunction in retinal capillaries secondary to NOTCH3 mutations and hypoperfusion in the DRP may cause nutritional deficiency in the synaptic connections of the retinal elements. In this case series choroidal vessels are affected in CADASIL patients [71]. These results are in line with previous OCT studies demonstrating increased wall thicknesses and outer diameters of arterial and venous retinal vessels [72]. Interestingly, retinal vessel changes may be correlated to brain MRI findings, highlighting the possible role of retinal changes as biomarker of the disease [73]. These results, pointing to a reduced retinal vessel density in CADASIL, are a confirmation of previous studies demonstrating by fractal analysis a reduced retinal vessel branching in CADASIL [74].

14.7 Wolfram Syndrome

Wolfram syndrome (WS) was first described in 1938 [75]. It is a rare neurodegenerative disorder characterized by the occurrence of diabetes mellitus and optic atrophy starting in childhood and a variable association of diabetes insipidus, other endocrinopathies, deafness, cerebellar ataxia, neurogenic bladder, cardiomyopathy

and psychiatric disturbances [76]. In fact, it is also known as DIDMOAD (Diabetes Insipidus, Diabetes Mellitus, Optic Atrophy) [77, 78]. Usually diabetes is the first sign of the disease. Optic atrophy appears in the first-second decade of life and it is in most cases severe [77, 79]. Wolfram's disease is due to mutations in the wolframin gene (*WFS1*) [80] and in the large majority of cases is inherited in an autosomal recessive fashion, but autosomal dominant inheritance has also been reported [81]. In these latter cases optic atrophy can be milder [81] and can be associated with deafness without diabetes [82]. Autosomal dominant mutations in the *WFS1* gene have been associated also with non-syndromic deafness [83], diabetes [84] and cataract [85]. Neuropathological studies reported atrophy of the optic nerve, chiasm, lateral geniculate nucleus, optic tracts and occipital cortex in WS [86–90].

A few OCT studies are available for WS. In a case report, spectral domain OCT documented a diffuse optic atrophy more evident in the superior and inferior quadrants in a 21 year-old male [91]. Bucca and coauthors reported time-domain findings in a 13 year-old female showing loss of retinal nerve fibers in the temporal quadrant [92]. More recently, Grenier and coauthors reported OCT findings in a case series of 15 WS cases carrying both autosomal recessive-ar (11 cases, 8 with diabetes and 3 without diabetes) and 4 autosomal dominant-ad *WFS1* mutations with hearing loss. Using SD-OCT, the authors showed that RNFL loss was more profound in the group with syndromic ar-WS compared to the WS cases without diabetes, especially in the inferior sectors. The comparison of ar-WS cases with ad-WS cases by time-domain OCT revealed a more severe RNFL thinning in the ar-WS group in both the superior and inferior quadrants [93].

In a pediatric case series of 12 genetically confirmed WS cases, the authors reported a significant reduction in the WS cases compared with individual with type 1 diabetes and controls of OCT parameters (including average and single quadrants RNFL thickness, macular full-thickness and macular ganglion cell layer/inner plexiform layer) especially in the superior and inferior sectors and brain MRI visual pathway measurements (intraorbital and intracranial thickness of the optical nerve, as well as the optic chiasm and visual tracts). Interestingly, in this case series some optic nerve parameters measured by MRI such as the thickness of the intraorbital parts of the optic nerves in WS cases correlated with superior RNFL thickness of the optic nerve evaluated by OCT [94].

Another interesting OCT finding in 8 ad-WS cases compared to 6 ar-WS cases is the presence of an abnormal reflectivity (lamination) of the outer plexiform layer, which may be related to the high wolframin expression in the retinal Müller cells [95]. This finding needs to be confirmed by larger clinical series.

Moreover, OCT parameters can be used as a marker of disease progression, as showed by a recent paper evaluating OCT changes over time in a group of 12 WS cases compared to type 1 diabetes patients. In this paper the WS cases were re-evaluated after a follow-up period of about 2 years and OCT measurements, including total thickness of the RNFL, average retinal thickness and total retinal volume, significantly decreased compared to the baseline investigation [96].

Finally, a postmortem study documented a specific pattern of optic atrophy predominantly involving the temporal and inferior quadrants, i.e. the papillomacular

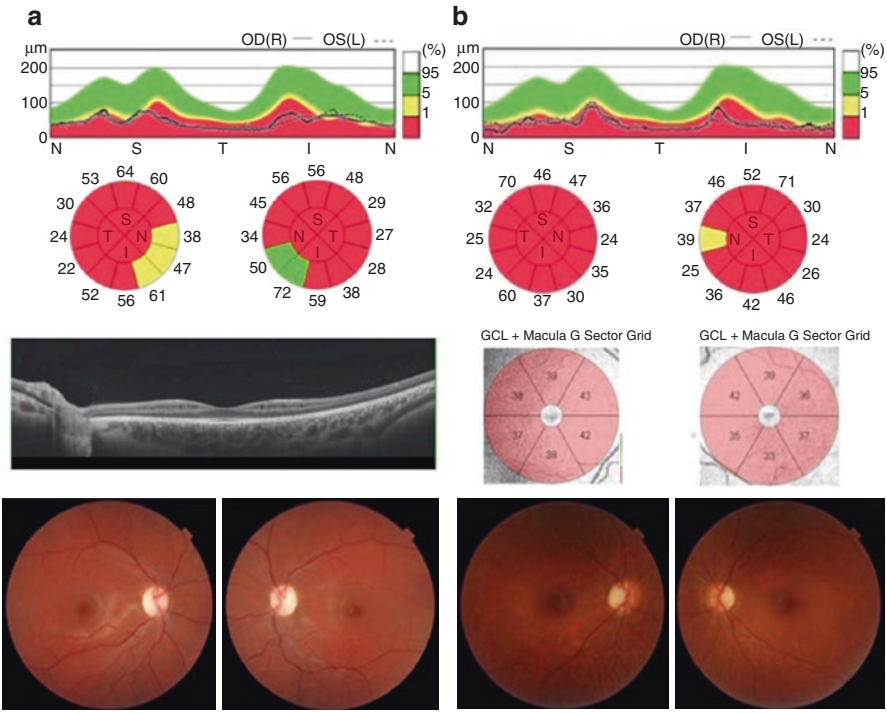

Fig. 14.4 (Wolfram) (**a**) This is a 18 year-old female, born from consanguineous parents, started complaining visual loss during childhood. She did not suffer diabetes. Visual acuity is 4/10 in RE and 3.2/10 in LE. Visual fields show a generalized defect (inf > nasal). OCT reveals diffuse RNFL thinning with relative nasal sparing and perimacular inner nuclear layer cysts. Fundus oculi images show a diffuse optic nerve pallor. (**b**) This is a 27-year-old female. She suffered diabetes mellitus since she was 10 year now on insulin therapy. Optic atrophy was noticed when she was 15 years. Visual acuity is 2.5/10 in the RE and 4/10 in the LE. OCT demonstrates diffuse RNFL thinning, as evident also at GCC. Fundus oculi images show bilateral temporal pallor

bundle of the optic nerve, in a WS case. This pattern resembles that described in mitochondrial optic neuropathies [90].

We here show the OCT findings of two WS patients (Fig. 14.4). A brief summary of their clinical history is reported below and ophthalmological findings are illustrated in Fig. 14.4.

14.7.1 Case 1

This is a 18 year-old female, born from consanguineous parents, started complaining visual loss during childhood. She did not suffer diabetes. Genetic analysis revealed the presence of the homozygous c.1553T>A mutation (p.M518K) in the *WFS1* gene. Lactic acid levels after standardized exercise were abnormally elevated. Muscle biopsy was histologically normal. Brain MRI and spectroscopy were normal.

14.7.2 Case 2

This is a 27 year-old female. She presented growth hormone deficiency at 8 years of age and diabetes mellitus at 10 year-old. She suffered from migraine since the age of 17. Genetic analysis showed the presence of compound heterozygous mutations c.409_426dup16 and c.2104 G>A in the *WFS1* gene. Brain MRI at 22 years showed microstructural degenerative cerebellar changes (middle cerebellar peduncles and emispheres). Optic atrophy was noticed when she was 15 years.

14.8 Autosomal Recessive Spastic Ataxia of Charlevoix-Saguenay (ARSACS)

Autosomal recessive spastic ataxia of Charlevoix-Saguenay (ARSACS) is a complex hereditary neurodegenerative disorder characterized by early childhood-onset cerebellar ataxia [97], peripheral neuropathy [98] and pyramidal tract signs [99, 100].

The name of the disease derives from its high prevalence, as a result of a founder effect, in the French-Canadian population of the Charlevoix-Saguenay region in the northeast of Quebec. After these initial reports ARSACS was also described in other countries and ethnic groups worldwide [101, 102].

ARSACS is due to mutations in the *SACS* gene, which were first identified by Engert and coauthors in 2000. The *SACS* gene is located on chromosome 13q12.12 and encodes the protein sacsin with a chaperone activity [102–105]. Sacsin is required for normal mitochondrial dynamics, and loss of function of this protein can result in an altered balance between mitochondrial fusion and fission [105, 106].

Furthermore, a recent study on a sacsin-knockout mouse model described a disruption of mitochondrial fission/fusion dynamics [106].

The majority of ARSACS patients show early ocular signs including the alteration of smooth ocular pursuit (horizontal gaze-evoked nystagmus) and the presence of prominent myelinated fibers radiating from the optic disc. These myelinated fibers are visible ophthalmoscopically and were considered the main clinical manifestations of ARSACS. However, there is phenotypic variability and the presence of myelinated fibers was rarely described in non-Quebec patients [107–114].

In the original characterization of ARSACS the authors described yellow streaks of hypermyelinated fibers that focally embed the retinal vessels, emanating radially from the edges of the optic disc [101]. In recent years, with the advent of new and more sophisticated quantitative retinal imaging technologies, the nature of the myelinated fibers in ARSACS has been debated.

In 2011, different OCT studies demonstrated that the typical ophthalmoscopic appearance in ARSACS patients is due to the increased hyper-reflectivity and thickness of the peripapillary RNFL and not to the presence of myelinated fibers [115–117]. Vingolo and coauthors [115] showed that the absence of shadowing behind the fibers in the OCT of ARSACS patients differentiates them from subjects with persistent myelinated fibers. In the latter, in fact, OCT clearly revealed a posterior

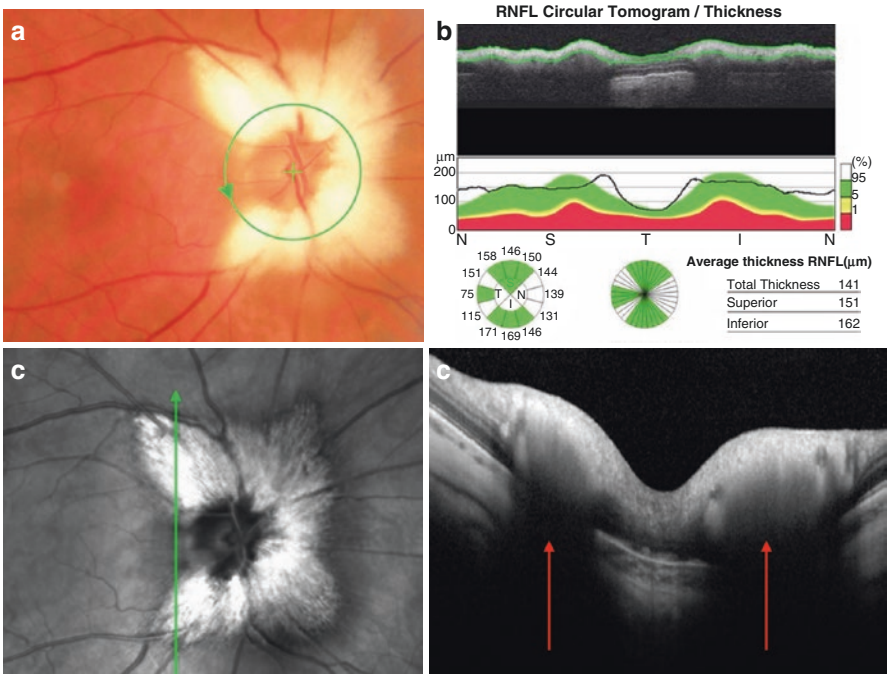

Fig. 14.5 OCT findings in persistent myelinated fibers. (**a**) Fundus photography of peripapillar myelin fibers. (**b**, **c**) Thickening of the peripapillar retinal fibers hiding the deep layers of retina (red arrow)

shadowing, due to the hyper-reflectivity and consequent "shield-effect" of the myelinated areas, which does not allow the OCT infrared laser to enter into the retina (Fig. 14.5).

The thickening of the retinal fibers can overcome the peripapillary region and reach the macula. Thus, the average macular thickness (mainly in nasal quadrant) and the average foveolar thickness may be increased in ARSACS patients [117]. Moreover, in 2016, by means of Spectral Domain-OCT (SD-OCT), Shah and coauthors, describing the characteristics of the fovea in an ARSAC patient, detected the incursion of inner retinal layers upon the foveal region leading to the lost of pit, exactly resembling the abnormality of development as seen in grade 2 foveal hypoplasia [118] (Fig. 14.6).

Also the OCT Angiography (Angio-OCT) of the ONH highlights the increase of vessel density in the radial peripapillary capillary plexus (RPC) probably due to the increased metabolic demand of the hypertrophic fibers (Fig. 14.7).

Recently Parkinson and coauthor, studying a large cohort of ARSACS patients found an inverse correlation between peripapillary RNFL thickness and both age at examination and age at onset; however, a significant correlation between the average peripapillary RNFL thickness and disease duration was not found [119].

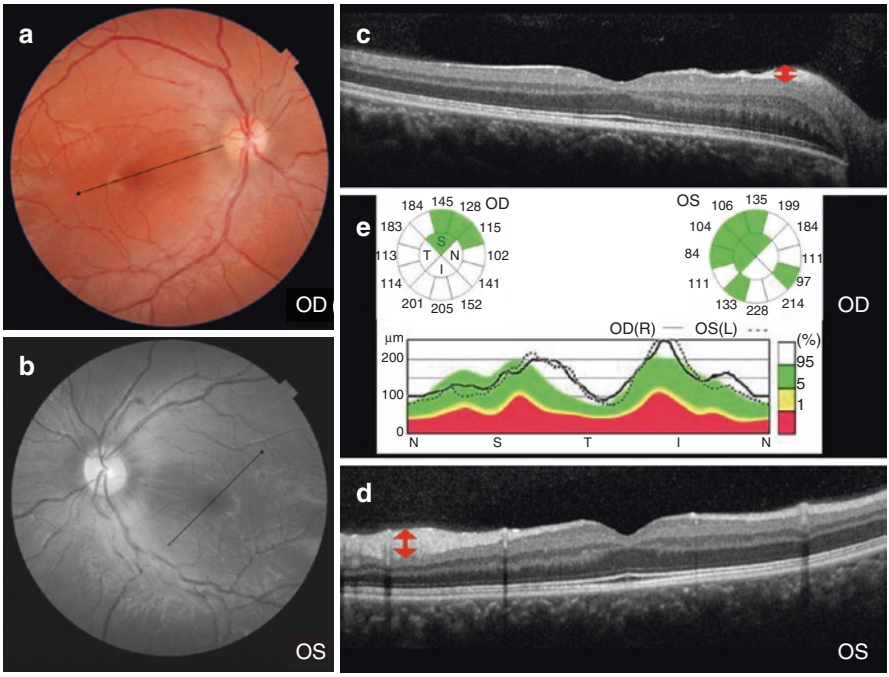

Fig. 14.6 OCT findings in a ARSACS patient. This is a 25-year old female carrying mutations in the *SACS* gene located on chromosome 13q12.12p. Visual acuity is 10/10 bilaterally. (**a**, **b**) Color and red-free fundus photograph. (**c**, **d**) OCT scans through the fovea reveal the hypertrophia of the nerve fiber layer (red arrows) and the incursion of inner retinal layers upon the foveal region as seen in grade 2 foveal hypoplasia (**e**) Increased thickness of peripapillar RNFL predominant in upper and lower temporal sectors

Typically, visual acuity is normal or rarely slightly reduced, without any central visual field defects (only mild and peripheral visual defects are reported). These findings overall support the absence of myelin deposition in the retina of these patients, given that the presence of myelin, would have caused more evident visual field defects as blind spot enlargement [120].

Concerning the ARSACS asymptomatic carriers, the results of two recent studies have been inconsistent and it is unclear whether or not there is some degree of RNFL hypertophy in individuals carrying heterozygous SACS gene mutations [119, 121].

Thus, it is preferable to use the term "retinal nerve fiber hypertrophy" [116] to define the retinal aspect of patients with ARSACS. In fact, the recent OCT findings, at least among non-Quebec patients, suggest that retinal hypermyelination has been used inappropriately to describe the striated appearance of a thickened RNFL around the optic discs in ARSACS patients [122]. Yu-Wai-Man and coauthors in 2013 have proposed the speculative hypothesis that the RNFL thickening in ARSACS could be related to the axoplasmic stasis within the long axons of the retinal ganglion cells as they converge to form the optic nerve in the anatomically tight region of the lamina cribrosa [122].

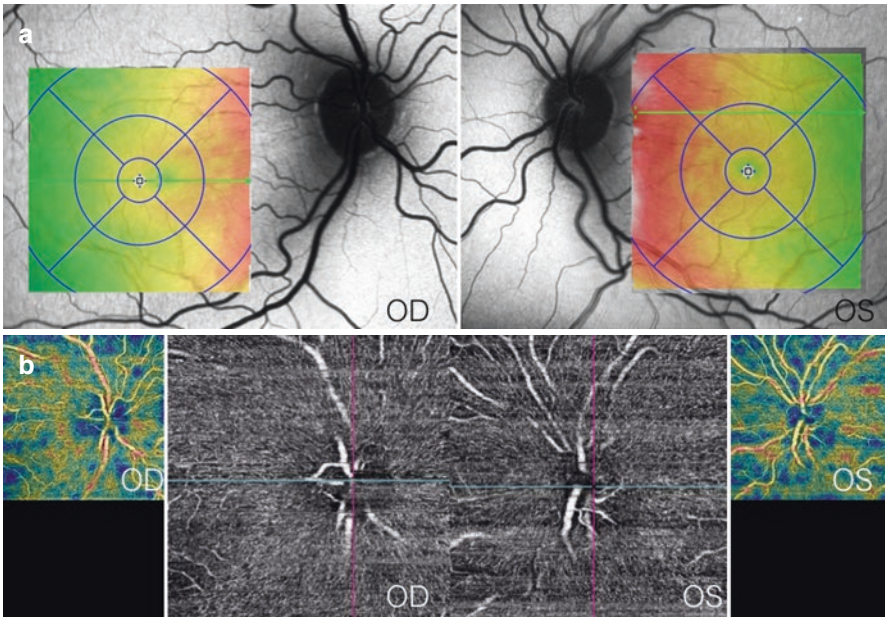

Fig. 14.7 AF and Angio-OCT findings in a ARSACS patient. (same patient as in Fig. 14.6). (**a**) Fundus autofluorescence with superimposed the ETDR thickness map shows a shadowing of the AF signal and a thickening in the OCT map in the area of the RNFL hypertrophy. (**b**) Angio-OCT of the ONH shows an increase of the numbers of the radial peripapillary capillaries (RPC)

14.9 Spinocerebellar Ataxias (SCAs)

Spinocerebellar ataxias (SCAs) are a genetically heterogeneous group of autosomal dominant neurodegenerative disorders characterized by ataxia, ocular motor abnormalities, and variable other neurological features, such as pyramidal tract, basal ganglia or brainstem dysfunction [123, 124]. The SCAs are classified on the basis of the genotype and currently include up to 40 genetically distinct entities [125]. SCA1, 2, 3, and 6, the most common ones, are caused by a trinucleotide CAG repeat expansion encoding glutamine in four unrelated proteins. SCA1, 2, and 3 are characterized by cerebellar degeneration and variable degrees of involvement of other central nervous system regions, whereas SCA6 is associated with a nearly pure cerebellar atrophy [123].

Abnormal afferent visual testing and optic atrophy have been described as a feature of SC1, SCA2 and SCA3 [126, 127]. Rarely, SCA2 is also associated with retinitis pigmentosa, most notably in the infantile form with extremely expanded CAG repeats [128], and pigmentary retinopathy has been reported in a patient homozygous for a pathological repeat expansion in the SCA6 gene [129].

Unlike other SCAs, patients with SCA7 exhibit a spectrum of severity of retinal disease from mild to severe dysfunction. Early functional abnormalities occur in both cones and rods, but greater centrally than peripherally [130, 131].

14.10 Spinocerebellar Ataxia Type 2-3-6 (SCA2-3-6)

Pula et al. in a spectral-domain OCT study reported in 29 SCA and cerebellar multisystem atrophy patients (SCA1-2-3-6 and MSA-C) a significant reduction of the peripapillar RNFL thickness for SCA2 and SCA3 patients only. This RNFL thinning correlated with the severity of the disease (Scale for the Assessment and Rating of Ataxia, SARA score) [132].

Another study by Alvarez and colleagues [133] demonstrated a significant reduction of the average RNFL thickness in nine SCA3 patients compared to age- and sex-matched controls. There was a reduction in the RNFL thickness in all quadrants except the temporal one, preserved in all eyes. Therefore, papillomacular bundle probably is not primarily involved in SCA-3 and consequently visual acuity is preserved in these patients (mean BCVA 20/25 and normal colour vision in all patients, except for the one with congenital dyscromatopsia). RNFL thickness was inversely correlated to SARA score. The mean macular thickness was lower compared to the control group only in two eyes (11.11%). In four patients, (eight eyes) OCT studies were performed with an average follow-up of 14.25 months, and in five eyes (62.50%) there was a trend towards a RNFL thickness reduction. Thus, the authors concluded that the pattern of the optic nerve involvement in SCA-3 is more similar to that observed in Alzheimer's and Parkinson's disease than to SCA-1 and toxic or mitochondrial optic nerve diseases where there is a preferential involvement of the papillo-macular bundle [133].

14.11 Spinocerebellar Ataxia Type 1 (SCA1)

Spinocerebellar ataxia type 1 (SCA1) is an autosomal dominantly inherited, late-onset neurodegenerative disease primarily affecting the cerebellar cortex and brainstem. Affected patients suffer from disturbed motor coordination, slurred speech, dysphagia, spasticity, extrapyramidal movements such as dystonia or chorea, cerebellar oculomotor disturbances, ophthalmoparesis, saccade slowing and cognitive impairment [134].

SCA1 is due to a CAG-repeat expansion of variable length reaching between 39 and 83 repeats encoding for a prolonged polyglutamine chain in the *ATXN1* gene on chromosome 6p23 encoding for the ataxin1 protein [134].

In SCA1 patients, besides the well-described cerebellar oculomotor abnormalities, there is also evidence of ocular pathology. There is evidence of visual acuity reduction, color vision impairment and central scotoma or contraction of visual fields [135, 136]. In some case series there is evidence of worsening of ocular symptoms with disease duration [137, 138]. The reduced visual acuity in SCA1 has been

attributed to optic atrophy, which was first described at fundus examination [138]. Optic nerve involvement was also suggested by abnormal VEP findings in SCA1 patients [139, 140]. However, VEPs were normal in 40–50% of SCA1 patients and retinal or optic nerve pathology was not consistently reported in SCA1 [141].

Stricker et al. [142], in a series of 9 SCA1 subjects compared to age- and sex-matched controls, demonstrated with OCT a pattern of temporal atrophy of the RNFL in most of the patients, suggesting a preferential involvement of the papillo-macular bundle. Segmentation analysis of the retina confirmed temporal RNFL thickness reduction whereas there was no significant difference in the average ganglion cell layer, inner and outer plexiform layer, photoreceptor layer and pigment epithelium. SCA1 patients showed a reduction in visual acuity and average RNFL thickness compared to healthy controls (84.0 μm vs. 97.2 μm). RNFL thinning was predominant and significant in temporal sectors ($p < 0.001$,) and was not found in nasal sectors. OCT findings were correlated with disease duration and disease severity measured by SARA score. The patient with the longest disease duration and highest SARA score showed additional severe macular atrophy, indicating that, at a later disease stage, nerve fiber atrophy could lead to ganglion cell degeneration and consecutively to macular volume reduction. Differently, VEP P100 latencies were not significantly different between SCA1 patients and controls [142].

The authors speculated that the selective temporal RNFL involvement could be explained by a differential vulnerability of the parvocellular axons to mutated ataxin1. In fact, the pattern of temporal RNFL thinning seen in these SCA1 patients could be due to localized oxidative dysfunction, which does not involve the magnocellular ganglion cell axons and the photoreceptors [142].

In 2013, two different groups [135, 136] simultaneously described a case series of six SCA1 patients presenting with progressive maculopathy and retinal dysfunction. The patients exhibited bilateral, progressive painless visual loss with macular drusen and mild pigmentary alterations at fundus examination.

In particular, Vaclavik and coauthors [136] showed two genetically confirmed SCA1 patients with bilateral areas of hypopigmented retinal pigment epithelium within the macula. Autofluorescence imaging revealed a central macular hyperautofluorescence surrounded by a ring of hypoautofluorescence. Spectral-domain OCT disclosed bilateral hyporeflective "foveal cavitation" corresponding to loss of the highly reflective inner segment/outer segment junction, as well as thinning of the outer nuclear layer. Outside the macula, the retina was within normal range. Fluorescein angiography showed small areas of patchy hyperfluorescence in the macula, corresponding to areas of depigmented retinal pigment epithelium without any leakage at later stages. Goldmann kinetic manual perimetry revealed a relative central scotoma bilaterally. The retinal function was tested using full-field ERG which was within normal limits under photopic and scotopic conditions. Multifocal electroretinography (mfERG) was not performed [136].

Two other patients with bilateral foveal cavities had OCT features similar to those reported previously in achromatopsia [143], and cone dystrophy [144], whereas RNFL thickness was not evaluated. Similarly, Lebranchu and coauthors reported a SCA1 family with maculopathy [135]. Four SCA1 patients showed

central scotoma in most of the eyes at visual field examination and visual acuities ranged between 20/20 and 20/200. Central retinal thinning with disorganized photoreceptor layers or foveal cavitation were found at OCT. Two patients showed mild temporal optic disc pallor at fundoscopy and thinning of the temporal RNFL at OCT, confirming the involvement of the papillomacular bundle [135]. In one patient, multifocal electroretinography (mfERG) revealed central retinal dysfunction. In these patients, OCT demonstrated alterations of the external layers of the fovea, suggesting a loss of structural integrity of the photoreceptors. The authors suggested that foveolar cavitation associated with the thinning of the whole macular area (including the surrounding perifoveolar retina) could be related to a cone dystrophy, as supported by the fact that a cluster of genes (*GUCA1A, PRPH2*) involved in macular diseases is located in a chromosome region (6p21.1) near the *SCA1* gene [135].

14.12 Spinocerebellar Ataxia Type 7 (SCA7)

Spinocerebellar ataxia type 7 (SCA7) is a progressive ataxia that is characterized by a high prevalence of retinal photoreceptor abnormalities. Recent studies suggest that the retinopathy of SCA7 is a cone-rod dystrophy [130, 131]. This degenerative retinopathy initially affects cones, and then progresses to cone–rod dystrophy [130]. Fundus examination demonstrates macular pigmentary changes, sometimes associated with mild temporal optic disc pallor [145]. The gene encodes for a protein (ataxin-7) widely expressed in the human retina [146]. This protein may interact with the function of CRX (cone–rod homeobox), a known transcription factor implicated in human cone–rod dystrophy [147].

In the last 10 years, with the advent of high-resolution spectral domain optical coherence tomography (SD-OCT), many studies demonstrated the presence of different grade of outer retinal atrophy with loss of the outer nuclear layer and ellipsoid zone in the central macula in SCA7 patients. Thus, the loss of the subfoveal ellipsoid zone corresponds to loss of cone photoreceptor cells which may be the earliest clinical sign of cone-rod dystrophy associated with SCA7 [148–152].

Manrique et al. [150] have described a case series of 7 patients with SCA7 in which the subjects with mild disease showed retinal thinning only at the fovea and subjects with more advanced disease tended to present retinal thinning also in the outer zone of the macula. Mean peripapillary RNFL thickness was decreased in all patients with sparing of the temporal quadrant until the advanced phases of the disease.

Furthermore, another study by Ahn et al. [151], using OCT and mfERG, revealed that retinal thinning extended outside the visible atrophic lesions and that the areas of functional deficits were greater than those of anatomic deficits.

Additionally, at a later stage of disease the maculopathy can evolve into a “bull’s eye” pattern [149]. The sparing of the temporal sector has been discussed as a possible result of the relative sparing of the inner macula around the central fovea associated with normal ganglion cell layer thickness at an earlier disease stage [151, 153].

14.13 Spinocerebellar Ataxia Type 10 (SCA10)

SCA 10 is caused by a pentanucleotide (ATTCT) repeat expansion on chromosome 22q13-qter. The SCA10 patients can present a purely cerebellar syndrome or a cerebellar syndrome concomitantly with epilepsy, polyneuropathy, and hematologic heart and liver conditions [154]. SCA10 shows a less aggressive clinical course than SCA3.

In 2017, Spina Tensini and coauthors used OCT to compare peripapillary RNFL and macular GCL thickness in patients with SCA3 and those with SCA10. They confirmed the reduction of the RNFL thickness in all quadrants but the temporal one in SCA3 patients and moreover they found RNFL thicker in SCA10 ($p > 0.05$) without any correlation between size of expansion, Scale for the Assessment and Rating of Ataxia (SARA), and RNFL or GCL thickness in SCA10 patients. These OCT structural findings are in accordance with the clinical course of SCA10, less aggressive than other SCAs [155].

14.14 Conclusions

In summary, OCT is a useful tool for investigating optic nerve and retinal involvement in many rare neurological disorders. Up to now, only a limited number of diseases have been extensively studied, as reported in this chapter. Single case reports with OCT findings are available for other rare neurological disorders such as Charcot-Marie-Tooth type 2A [156], and the X-linked adrenoleukodystrophy [157]. Thus, the application of this technique to larger case series will allow a better characterization of the ocular phenotype in these and other neurological diseases.

References

1. Collins A. Clinical neurogenetics: friedreich ataxia. Neurol Clin. 2013;31:1095–120.
2. Parkinson MH, Boesch S, Nachbauer W, Mariotti C, Giunti P. Clinical features of Friedreich's ataxia: classical and atypical phenotypes. J Neurochem. 2013;126(Suppl 1):103–17.
3. Campuzano V, Montermini L, Moltò MD, Pianese L, Cossée M, Cavalcanti F, et al. Friedreich's ataxia: autosomal recessive disease caused by an intronic GAA triplet repeat expansion. Science. 1996;271:1423–7.
4. Tan G, Napoli E, Taroni F, Cortopassi G. Decreased expression of genes involved in sulfur amino acid metabolism in frataxin-deficient cells. Hum Mol Genet. 2003;12:1699–711.
5. Shan Y, Napoli E, Cortopassi G. Mitochondrial frataxin interacts with ISD11 of the NFS1/ISCU complex and multiple mitochondrial chaperones. Hum Mol Genet. 2007;16:929–41.
6. Martelli A, Puccio H. Dysregulation of cellular iron metabolism in Friedreich ataxia: from primary iron-sulfur cluster deficit to mitochondrial iron accumulation. Front Pharmacol. 2014;5:130.
7. Rötig A, de Lonlay P, Chretien D, Foury F, Koenig M, Sidi D, et al. Aconitase and mitochondrial iron-sulphur protein deficiency in Friedreich ataxia. Nat Genet. 1997;17:215–7.
8. Lodi R, Cooper JM, Bradley JL, Manners D, Styles P, Taylor DJ, et al. Deficit of in vivo mitochondrial ATP production in patients with Friedreich ataxia. Proc Natl Acad Sci U S A. 1999;96:11492–5.

9. Bolinches-Amorós A, Mollá B, Pla-Martín D, Palau F, González-Cabo P. Mitochondrial dysfunction induced by frataxin deficiency is associated with cellular senescence and abnormal calcium metabolism. Front Cell Neurosci. 2014;8:124.
10. Babcock M, de Silva D, Oaks R, Davis-Kaplan S, Jiralerspong S, Montermini L, et al. Regulation of mitochondrial iron accumulation by Yfh1p, a putative homolog of frataxin. Science. 1997;276:1709–12.
11. Wong A, Yang J, Cavadini P, Gellera C, Lonnerdal B, Taroni F, et al. The Friedreich's ataxia mutation confers cellular sensitivity to oxidant stress which is rescued by chelators of iron and calcium and inhibitors of apoptosis. Hum Mol Genet. 1999;8:425–30.
12. Gomes CM, Santos R. Neurodegeneration in Friedreich's ataxia: from defective frataxin to oxidative stress. Oxidative Med Cell Longev. 2013;2013:487534.
13. Kersten HM, Roxburgh RH, Danesh-Meyer HV. Ophthalmic manifestations of inherited neurodegenerative disorders. Nat Rev Neurol. 2014;10:349–62.
14. Andermann E, Remillard GM, Goyer C, Blitzer L, Andermann F, Barbeau A. Genetic and family studies in Friedreich's ataxia. Can J Neurol Sci. 1976;3:287–301.
15. Carroll WM, Kriss A, Baraitser M, Barrett G, Halliday AM. The incidence and nature of visual pathway involvement in Friedreich's ataxia. A clinical and visual evoked potential study of 22 patients. Brain. 1980;103:413–34.
16. Fortuna F, Barboni P, Liguori R, Valentino ML, Savini G, Gellera C, et al. Visual system involvement in patients with Friedreich's ataxia. Brain. 2009;132:116–23.
17. Noval S, Contreras I, Sanz-Gallego I, Manrique RK, Arpa J. Ophthalmic features of Friedreich ataxia. Eye. 2012;26:315–20.
18. Seyer LA, Galetta K, Wilson J, Sakai R, Perlman S, Mathews K, et al. Analysis of the visual system in Friedreich ataxia. J Neurol. 2013;260:2362–9.
19. Dağ E, Örnek N, Örnek K, Erbahçeci-Timur IE. Optical coherence tomography and visual field findings in patients with Friedreich ataxia. J Neuroophthalmol. 2014;34:118–21.
20. Barboni P, Carbonelli M, Savini G, Ramos Cdo V, Carta A, Berezovsky A, et al. Natural history of Leber's hereditary optic neuropathy: longitudinal analysis of the retinal nerve fiber layer by optical coherence tomography. Ophthalmology. 2010;117:623–7.
21. Cotman SL, Karaa A, Staropoli JF, Sims KB. Neuronal ceroid lipofuscinosis: impact of recent genetic advances and expansion of the clinicopathologic spectrum. Curr Neurol Neurosci Rep. 2013;13:366.
22. Wheeler RB, Schlie M, Kominami E, Gerhard L, Goebel HH. Neuronal ceroid lipofuscinosis: late infantile or Jansky Bielschowsky type--re-revisited. Acta Neuropathol. 2001;102:485–8.
23. Bennett MJ, Rakheja D. The neuronal ceroid-lipofuscinoses. Dev Disabil Res Rev. 2013;17:254–9.
24. Hainsworth DP, Liu GT, Hamm CW, Katz ML. Funduscopic and angiographic appearance in the neuronal ceroid lipofuscinoses. Retina. 2009;29:657–68.
25. Worgall S, Kekatpure MV, Heier L, Ballon D, Dyke JP, Shungu D, et al. Neurological deterioration in late infantile neuronal ceroid lipofuscinosis. Neurology. 2007;69:521–35.
26. Goebel HH, Zeman W, Damaske E. An ultrastructural study of the retina in the Jansky-Bielschowsky type of neuronal ceroid-lipofuscinosis. Am J Ophthalmol. 1977;83:70–9.
27. Weleber RG. The dystrophic retina in multisystem disorders: the electroretinogram in neuronal ceroid lipofuscinoses. Eye. 1998;12:580–90.
28. Sappington RM, Pearce DA, Calkins DJ. Optic nerve degeneration in a murine model of juvenile ceroid lipofuscinosis. Invest Ophthalmol Vis Sci. 2003;44:3725–31.
29. Weimer JM, Custer AW, Benedict JW, Alexander NA, Kingsley E, Federoff HJ, et al. Visual deficits in a mouse model of Batten disease are the result of optic nerve degeneration and loss of dorsal lateral geniculate thalamic neurons. Neurobiol Dis. 2006;22:284–93.
30. Mahmood F, Fu S, Cooke J, Wilson SW, Cooper JD, Russell C. A zebrafish model of CLN2 disease is deficient in tripeptidyl peptidase 1 and displays progressive neurodegeneration accompanied by a reduction in proliferation. Brain. 2013;136:1488–507.
31. Groh J, Stadler D, Buttmann M, Martini R. Non-invasive assessment of retinal alterations in mouse models of infantile and juvenile neuronal ceroid lipofuscinosis by spectral domain optical coherence tomography. Acta Neuropathol Commun. 2014;2:54.

32. Nardocci N, Verga ML, Binelli S, Zorzi G, Angelini L, Bugiani O. Neuronal ceroid-lipofuscinosis: a clinical and morphological study of 19 patients. Am J Med Genet. 1995;57:137–41.
33. Orlin A, Sondhi D, Witmer MT, Wessel MM, Mezey JG, Kaminsky SM, et al. Spectrum of ocular manifestations in CLN2-associated batten (Jansky-Bielschowsky) disease correlate with advancing age and deteriorating neurological function. PLoS One. 2013;8:e73128.
34. Wisniewski KE, Zhong N, Philippart M. Pheno/genotypic correlations of neuronal ceroid lipofuscinoses. Neurology. 2001;57(4):576–81.
35. Ku CA, Hull S, Arno G, Vincent A, Carss K, Kayton R, Weeks D, Anderson GW, Geraets R, Parker C, Pearce DA, Michaelides M, MacLaren RE, Robson AG, Holder GE, Heon E, Raymond FL, Moore AT, Webster AR, Pennesi ME. Detailed clinical phenotype and molecular genetic findings in CLN3-associated isolated retinal degeneration. JAMA Ophthalmol. 2017;135(7):749–60.
36. Preising MN, Abura M, Jäger M, Wassill KH, Lorenz B. Ocular morphology and function in juvenile neuronal ceroid lipofuscinosis (CLN3) in the first decade of life. Ophthalmic Genet. 2017;38(3):252–9.
37. Dulz S, Wagenfeld L, Nickel M, et al. Novel morphological macular findings in juvenile CLN3 disease. Br J Ophthalmol. 2016;100:824–8.
38. Klein CJ, Botuyan MV, Wu Y, Ward CJ, Nicholson GA, Hammans S, et al. Mutations in DNMT1 cause hereditary sensory neuropathy with dementia and hearing loss. Nat Genet. 2011;43:595–600.
39. Winkelmann J, Lin L, Schormair B, Kornum BR, Faraco J, Plazzi G, et al. Mutations in DNMT1 cause autosomal dominant cerebellar ataxia, deafness and narcolepsy. Hum Mol Genet. 2012;21:2205–10.
40. Moghadam KK, Pizza F, La Morgia C, Franceschini C, Tonon C, Lodi R, et al. Narcolepsy is a common phenotype in HSAN IE and ADCA-DN. Brain. 2014;137:1643–55.
41. Melberg A, Hetta J, Dahl N, Nennesmo I, Bengtsson M, Wibom R, et al. Autosomal dominant cerebellar ataxia deafness and narcolepsy. J Neurol Sci. 1995;134:119–29.
42. Lundberg PO, Wranne I, Brun A. Family with optic atrophy and neurological symptoms. Acta Neurol Scand. 1967;43:87–105.
43. Takasugi M, Yagi S, Hirabayashi K, Shiota K. DNA methylation status of nuclear-encoded mitochondrial genes underlies the tissue-dependent mitochondrial functions. BMC Genomics. 2010;11:481.
44. Shock LS, Thakkar PV, Peterson EJ, Moran RG, Taylor SM. DNA methyltransferase 1, cytosine methylation, and cytosine hydroxymethylation in mammalian mitochondria. Proc Natl Acad Sci U S A. 2011;108:3630–5.
45. Bellizzi D, D'Aquila P, Scafone T, Giordano M, Riso V, Riccio A, et al. The control region of mitochondrial DNA shows an unusual CpG and non-CpG methylation pattern. DNA Res. 2013;20:537–47.
46. Singh RK, Mallela RK, Hayes A, Dunham NR, Hedden ME, Enke RA, Fariss RN, Sternberg H, West MD, Nasonkin IO. Dnmt1, Dnmt3a and Dnmt3b cooperate in photoreceptor and outer plexiform layer development in the mammalian retina. Exp Eye Res. 2017;159:132–46.
47. Lo Giudice T, Lombardi F, Santorelli FM, Kawarai T, Orlacchio A. Hereditary spastic paraplegia: clinical-genetic characteristics and evolving molecular mechanisms. Exp Neurol. 2014;261C:518–39.
48. Casari G, De Fusco M, Ciarmatori S, Zeviani M, Mora M, Fernandez P, et al. Spastic paraplegia and OXPHOS impairment caused by mutations in paraplegin, a nuclear-encoded mitochondrial metalloprotease. Cell. 1998;93:973–83.
49. De Michele G, De Fusco M, Cavalcanti F, Filla A, Marconi R, Volpe G, et al. A new locus for autosomal recessive hereditary spastic paraplegia maps to chromosome 16q24.3. Am J Hum Genet. 1998;63:135–9.
50. Rugarli EI, Langer T. Translating m-AAA protease function in mitochondria to hereditary spastic paraplegia. Trends Mol Med. 2006;12:262–9.

51. Nolden M, Ehses S, Koppen M, Bernacchia A, Rugarli EI, Langer T. The m-AAA protease defective in hereditary spastic paraplegia controls ribosome assembly in mitochondria. Cell. 2005;123:277–89.
52. Atorino L, Silvestri L, Koppen M, Cassina L, Ballabio A, Marconi R, et al. Loss of m-AAA protease in mitochondria causes complex I deficiency and increased sensitivity to oxidative stress in hereditary spastic paraplegia. J Cell Biol. 2003;163:777–87.
53. McDermott CJ, Dayaratne RK, Tomkins J, Lusher ME, Lindsey JC, Johnson MA, et al. Paraplegin gene analysis in hereditary spastic paraparesis (HSP) pedigrees in Northeast England. Neurology. 2001;56:467–71.
54. Ehses S, Raschke I, Mancuso G, Bernacchia A, Geimer S, Tondera D, et al. Regulation of OPA1 processing and mitochondrial fusion by m-AAA protease isoenzymes and OMA1. J Cell Biol. 2009;187:1023–36.
55. Klebe S, Depienne C, Gerber S, Challe G, Anheim M, Charles P, et al. Spastic paraplegia gene 7 in patients with spasticity and/or optic neuropathy. Brain. 2012;135:2980–93.
56. van Gassen KL, van der Heijden CD, de Bot ST, den Dunnen WF, van den Berg LH, Verschuuren-Bemelmans CC, et al. Genotype-phenotype correlations in spastic paraplegia type 7: a study in a large Dutch cohort. Brain. 2012;135:2994–3004.
57. Marcotulli C, Leonardi L, Tessa A, De Negris AM, Cornia R, Pierallini A, et al. Early-onset optic neuropathy as initial clinical presentation in SPG7. J Neurol. 2014;261:1820–1.
58. Wiethoff S, Zhour A, Schöls L, Fischer MD. Retinal nerve fibre layer loss in hereditary spastic paraplegias is restricted to complex phenotypes. BMC Neurol. 2012;12:143.
59. Chabriat H, Joutel A, Dichgans M, Tournier-Lasserve E, Bousser MG. Cadasil. Lancet Neurol. 2009;8:643–53.
60. O'Sullivan M, Jarosz JM, Martin RJ, Deasy N, Powell JF, Markus HS. MRI hyperintensities of the temporal lobe and external capsule in patients with CADASIL. Neurology. 2001;56:628–34.
61. Joutel A, Corpechot C, Ducros A, Vahedi K, Chabriat H, Mouton P, et al. Notch3 mutations in cerebral autosomal dominant arteriopathy with subcortical infarcts and leukoencephalopathy (CADASIL), a mendelian condition causing stroke and vascular dementia. Ann N Y Acad Sci. 1997;826:213–7.
62. Belin de Chantemèle EJ, Retailleau K, Pinaud F, Vessières E, Bocquet A, Guihot AL, et al. Notch3 is a major regulator of vascular tone in cerebral and tail resistance arteries. Arterioscler Thromb Vasc Biol. 2008;28:2216–24.
63. Robinson W, Galetta SL, McCluskey L, Forman MS, Balcer LJ. Retinal findings in cerebral autosomal dominant arteriopathy with subcortical infarcts and leukoencephalopathy (cadasil). Surv Ophthalmol. 2001;45:445–8.
64. Roine S, Harju M, Kivelä TT, Pöyhönen M, Nikoskelainen E, Tuisku S, et al. Ophthalmologic findings in cerebral autosomal dominant arteriopathy with subcortical infarcts and leukoencephalopathy: a cross-sectional study. Ophthalmology. 2006;113:1411–7.
65. Haritoglou C, Rudolph G, Hoops JP, Opherk C, Kampik A, Dichgans M. Retinal vascular abnormalities in CADASIL. Neurology. 2004;62:1202–5.
66. Pretegiani E, Rosini F, Dotti MT, Bianchi S, Federico A, Rufa A. Visual system involvement in CADASIL. J Stroke Cerebrovasc Dis. 2013;22:1377–84.
67. Parisi V, Pierelli F, Fattapposta F, Bianco F, Parisi L, Restuccia R, et al. Early visual function impairment in CADASIL. Neurology. 2003;60:2008–10.
68. Rufa A, Malandrini A, Dotti MT, Berti G, Salvadori C, Federico A. Typical pathological changes of CADASIL in the optic nerve. Neurol Sci. 2005;26:271–4.
69. Parisi V, Pierelli F, Coppola G, Restuccia R, Ferrazzoli D, Scassa C, et al. Reduction of optic nerve fiber layer thickness in CADASIL. Eur J Neurol. 2007;14:627–31.
70. Rufa A, Pretegiani E, Frezzotti P, De Stefano N, Cevenini G, Dotti MT, et al. Retinal nerve fiber layer thinning in CADASIL: an optical coherence tomography and MRI study. Cerebrovasc Dis. 2011;31:77–82.
71. Nelis P, Kleffner I, Burg MC, Clemens CR, Alnawaiseh M, Motte J, Marziniak M, Eter N, Alten F. OCT-angiography reveals reduced vessel density in the deep retinal plexus of CADASIL patients. Sci Rep. 2018;8(1):8148.

72. Alten F, Motte J, Ewering C, Osada N, Clemens CR, Kadas EM, Eter N, Paul F, Marziniak M. Multimodal retinal vessel analysis in CADASIL patients. PLoS One. 2014;9(11):e112311.
73. Fang XJ, Yu M, Wu Y, Zhang ZH, Wang WW, Wang ZX, Yuan Y. Study of enhanced depth imaging optical coherence tomography in cerebral autosomal dominant arteriopathy with subcortical infarcts and leukoencephalopathy. Chin Med J. 2017;130(9):1042–8.
74. Cavallari M, Falco T, Frontali M, Romano S, Bagnato F, Orzi F. Fractal analysis reveals reduced complexity of retinal vessels in CADASIL. PLoS One. 2011;6(4):e19150.
75. Wolfram D, Wagener HP. Diabetes mellitus and simple optic atrophy among siblings: report of four cases. Proc Staff Meet Mayo Clin. 1938;13:715–8.
76. Rigoli L, Di Bella C. Wolfram syndrome 1 and Wolfram syndrome 2. Curr Opin Pediatr. 2012;24:512–7.
77. Barrett TG, Poulton K, Bundey S. DIDMOAD syndrome; further studies and muscle biochemistry. J Inherit Metab Dis. 1995;18:218–20.
78. Barrett TG, Bundey SE. Wolfram (DIDMOAD) syndrome. J Med Genet. 1997;34:838–41.
79. Barrett TG, Bundey SE, Fielder AR, Good PA. Optic atrophy in Wolfram (DIDMOAD) syndrome. Eye. 1997;11:882–8.
80. Inoue H, Tanizawa Y, Wasson J, Behn P, Kalidas K, Bernal-Mizrachi E, et al. A gene encoding a transmembrane protein is mutated in patients with diabetes mellitus and optic atrophy (Wolfram syndrome). Nat Genet. 1998;20:143–8.
81. Eiberg H, Hansen L, Kjer B, Hansen T, Pedersen O, Bille M, et al. Autosomal dominant optic atrophy associated with hearing impairment and impaired glucose regulation caused by a missense mutation in the WFS1 gene. J Med Genet. 2006;43:435–40.
82. Rendtorff ND, Lodahl M, Boulahbel H, Johansen IR, Pandya A, Welch KO, et al. Identification of p.A684V missense mutation in the WFS1 gene as a frequent cause of autosomal dominant optic atrophy and hearing impairment. Am J Med Genet A. 2011;155A:1298–313.
83. Bai X, Lv H, Zhang F, Liu J, Fan Z, Xu L, et al. Identification of a novel missense mutation in the WFS1 gene as a cause of autosomal dominant nonsyndromic sensorineural hearing loss in all-frequencies. Am J Med Genet A. 2014;164:3052–60.
84. Bonnycastle LL, Chines PS, Hara T, Huyghe JR, Swift AJ, Heikinheimo P, et al. Autosomal dominant diabetes arising from a Wolfram syndrome 1 mutation. Diabetes. 2013;62:3943–50.
85. Berry V, Gregory-Evans C, Emmett W, Waseem N, Raby J, Prescott D, et al. Wolfram gene (WFS1) mutation causes autosomal dominant congenital nuclear cataract in humans. Eur J Hum Genet. 2013;21:1356–60.
86. Carson MJ, Slager UT, Steinberg RM. Simultaneous occurrence of diabetes mellitus, diabetes insipidus, and optic atrophy in a brother and sister. Am J Dis Child. 1977;131:1382–5.
87. Jackson MJ, Bindoff LA, Weber K, Wilson JN, Ince P, Alberti KG, et al. Biochemical and molecular studies of mitochondrial function in diabetes insipidus, diabetes mellitus, optic atrophy, and deafness. Diabetes Care. 1994;17:728–33.
88. Shannon P, Becker L, Deck J. Evidence of widespread axonal pathology in Wolfram syndrome. Acta Neuropathol. 1999;98:304–8.
89. Hilson JB, Merchant SN, Adams JC, Joseph JT. Wolfram syndrome: a clinicopathologic correlation. Acta Neuropathol. 2009;118:415–28.
90. Ross-Cisneros FN, Pan BX, Silva RA, Miller NR, Albini TA, Tranebjaerg L, et al. Optic nerve histopathology in a case of Wolfram syndrome: a mitochondrial pattern of axonal loss. Mitochondrion. 2013;13:841–5.
91. Bababeygy SR, Wang MY, Khaderi KR, Sadun AA. Visual improvement with the use of idebenone in the treatment of Wolfram syndrome. J Neuroophthalmol. 2012;32:386–9.
92. Bucca BC, Klingensmith G, Bennett JL. Wolfram syndrome: a rare optic neuropathy in youth with type 1 diabetes. Optom Vis Sci. 2011;88:E1383–90.
93. Grenier J, Meunier I, Daien V, Baudoin C, Halloy F, Bocquet B, Blanchet C, Delettre C, Esmenjaud E, Roubertie A, Lenaers G, Hamel CP. WFS1 in optic neuropathies: mutation findings in nonsyndromic optic atrophy and assessment of clinical severity. Ophthalmology. 2016;123(9):1989–98.

94. Zmyslowska A, Waszczykowska A, Baranska D, Stawiski K, Borowiec M, Jurowski P, Fendler W, Mlynarski W. Optical coherence tomography and magnetic resonance imaging visual pathway evaluation in Wolfram syndrome. Dev Med Child Neurol. 2019;61: 359–65.
95. Majander A, Bitner-Glindzicz M, Chan CM, Duncan HJ, Chinnery PF, Subash M, Keane PA, Webster AR, Moore AT, Michaelides M, Yu-Wai-Man P. Lamination of the outer plexiform layer in optic atrophy caused by dominant WFS1 mutations. Ophthalmology. 2016;123(7):1624–6.
96. Zmyslowska A, Fendler W, Waszczykowska A, Niwald A, Borowiec M, Jurowski P, Mlynarski W. Retinal thickness as a marker of disease progression in longitudinal observation of patients with Wolfram syndrome. Acta Diabetol. 2017;54(11):1019–24.
97. Bouhlal Y, Amouri R, El Euch-Fayeche G, Hentati F. Autosomal recessive spastic ataxia of Charlevoix-Saguenay: an overview. Parkinsonism Relat Disord. 2011;17:418–22.
98. Berciano J, García A, Infante J. Peripheral nerve involvement in hereditary cerebellar and multisystem degenerative disorders. Handb Clin Neurol. 2013;115:907–32.
99. Duquette A, Brais B, Bouchard JP, Mathieu J. Clinical presentation and early evolution of spastic ataxia of Charlevoix-Saguenay. Mov Disord. 2013;28:2011–4.
100. Baets J, Deconinck T, Smets K, Goossens D, Van den Bergh P, Dahan K, et al. Mutations in SACS cause atypical and late-onset forms of ARSACS. Neurology. 2010 28;75:1181–8.
101. Bouchard JP, Barbeau A, Bouchard R, Bouchard RW. Autosomal recessive spastic ataxia of Charlevoix-Saguenay. Can J Neurol Sci. 1978;5:61e9.
102. De Braekeleer M, Giasson F, Mathieu J, Roy M, Bouchard JP, Morgan K. Genetic epidemiology of autosomal recessive spastic ataxia of Charlevoixe-Saguenay in northeastern Quebec. Genet Epidemiol. 1993;10:17e25.
103. Engert JC, Bérubé P, Mercier J, Doré C, Lepage P, Ge B, Bouchard JP, Mathieu J, et al. ARSACS, a spastic ataxia common in northeastern Québec, is caused by mutations in a new gene encoding an 11.5-kb ORF. Nat Genet. 2000;24:120e5.
104. Cheetham ME, Caplan AJ. Structure, function and evolution of DnaJ: conservation and adaptation of chaperone function. Cell Stress Chaperones. 1998;3:28e36.
105. Parfitt DA, Michael GJ, Vermeulen EG, Prodromou NV, Webb TR, Gallo JM, et al. The ataxia protein sacsin is a functional co-chaperone that protects against polyglutamine-expanded ataxin-1. Hum Mol Genet. 2009;18:1556e65.
106. Girard M, Larivière R, Parfitt DA, Deane EC, Gaudet R, Nossova N, et al. Mitochondrial dysfunction and Purkinje cell loss in autosomal recessive spastic ataxia of Charlevoix-Saguenay (ARSACS). Proc Natl Acad Sci U S A. 2012;109:1661–6.
107. El Euch-Fayache G, Lalani I, Amouri R, Turki I, Ouahchi K, Hung WY, et al. Phenotypic features and genetic findings in sacsin-related autosomal recessive ataxia in Tunisia. Arch Neurol. 2003;60:982e8.
108. Grieco GS, Malandrini A, Comanducci G, Leuzzi V, Valoppi M, Tessa A, et al. Novel SACS mutations in autosomal recessive spastic ataxia of Charlevoixe-Saguenay type. Neurology. 2004;62:103e6.
109. Criscuolo C, Banfi S, Orio M, Gasparini P, Monticelli A, Scarano V, et al. A novel mutation in SACS gene in a family from southern Italy. Neurology. 2004;62:100e2.
110. Takiyama Y. Autosomal recessive spastic ataxia of Charlevoixe-Saguenay. Neuropathology. 2006;26:368e75.
111. Bouhlal Y, Zouari M, Kefi M, Ben Hamida C, Hentati F, Amouri R. Autosomal recessive ataxia caused by three distinct gene defects in a single consanguineous family. J Neurogenet. 2008;22:139e48.
112. Vermeer S, Meijer RP, Pijl BJ, Timmermans J, Cruysberg JR, Bos MM, et al. ARSACS in the Dutch population: a frequent cause of early-onset cerebellar ataxia. Neurogenetics. 2008;10:87.
113. Bouhlal Y, El Euch-Fayeche G, Hentati F, Amouri R. A novel SACS gene mutation in a Tunisian family. J Mol Neurosci. 2009;39:333e6.
114. Takiyama Y. Sacsinopathies: sacsin-related ataxia. Cerebellum. 2007;6:353–9.

115. Vingolo EM, Di Fabio R, Salvatore S, Greco G, Bertini E, Lezzi V, et al. Myelinated retinal fibers in autosomal recessive spastic ataxia of Charlevoix-Saguenay. Eur J Neurol. 2011;18:1187–90.
116. Pablo LE, Garcia-Martin E, Gazulla J, Larrosa JM, Ferreras A, Santorelli FM, et al. Retinal nerve fiber hypertrophy in ataxia of Charlevoix-Saguenay patients. Mol Vis. 2011;17:1871–6.
117. Desserre J, Devos D, Sautière BG, Debruyne P, Santorelli FM, Vuillaume I, et al. Thickening of peripapillar retinal fibers for the diagnosis of autosomal recessive spastic ataxia of Charlevoix-Saguenay. Cerebellum. 2011;10:758–62.
118. Shah CT, Ward TS, Matsumoto JA, et al. Foveal hypoplasia in autosomal recessive spastic ataxia of Charlevoix-Saguenay. J AAPOS. 2016;20(1):81–3.
119. Parkinson MH, Bartmann AP, Clayton LMS, et al. Optical coherence tomography in autosomal recessive spastic ataxia of Charlevoix-Saguenay. Brain. 2018;141(4):989–99.
120. Gazulla J, Benavente I, Vela AC, Marín MA, Pablo LE, Tessa A, Barrena MR, et al. New findings in the ataxia of Charlevoix-Saguenay. J Neurol. 2012;259:869–78.
121. Van Lint M, Hoornaert K, Ten Tusscher MPM. Retinal nerve fiber layer thickening in ARSACS carriers. J Neurol Sci. 2016;370:119–22.
122. Yu-Wai-Man P, Pyle A, Griffin H, Santibanez-Korev M, Chinnery PF. Abnormal retinal thickening is a common feature among patients with ARSACS-related phenotypes. Br J Ophthalmol. 2014;98:711–3.
123. Koeppen AH. The pathogenesis of spinocerebellar ataxia. Cerebellum. 2005;4:62–73.
124. Durr A. Autosomal dominant cerebellar ataxias: polyglutamine expansions and beyond. Lancet Neurol. 2010;9:885–94.
125. Mudwiler A, Shakkottai VG. Autosomal-dominant cerebellar ataxias. Handb Clin Neurol. 2018;147:173–85.
126. Pula JH, Gomez CM, Kattah JC. Ophthalmologic features of the common spinocerebellar ataxias. Curr Opin Ophthalmol. 2010;21:447–53.
127. Newman NJ, Biousse V. Hereditary optic neuropathies. Eye. 2004;18(11):1144–60.
128. Rufa A, Dotti MT, Galli L, Orrico A, Sicurelli F, Federico A. Spinocerebellar ataxia type 2 (SCA2) associated with retinal pigmentary degeneration. Eur Neurol. 2002;47:128–9.
129. Fukutake T, Kamitsukasa I, Arai K, Hattori T, Nakajima T. A patient homozygous for the SCA6 gene with retinitis pigmentosa. Clin Genet. 2002;61:375–9.
130. Aleman TS, Cideciyan AV, Volpe NJ, Stevanin G, Brice A, Jacobson SG. Spinocerebellar ataxia type 7 (SCA7) shows a cone-rod dystrophy phenotype. Exp Eye Res. 2002;74:737–45.
131. Abe T, Tsuda T, Yoshida M, Wada Y, Kano T, Itoyama Y, et al. Macular degeneration associated with aberrant expansion of trinucleotide repeat of the SCA7 gene in 2 Japanese families. Arch Ophthalmol. 2000;118:1415–21.
132. Pula JH, Towle VL, Staszak VM, Cao D, Bernard JT, Gomez CM. Retinal nerve fibre layer and macular thinning in spinocerebellar ataxia and cerebellar multisystem atrophy. Neuroophthalmology. 2011;35(3):108–14.
133. Alvarez G, Rey A, Sanchez-Dalmau FB, Muñoz E, Ríos J, Adán A. Optical coherence tomography findings in spinocerebellar ataxia-3. Eye. 2013;27:1376–81.
134. Schöls L, Bauer P, Schmidt T, Schulte T, Riess O. Autosomal dominant cerebellar ataxias: clinical features, genetics, and pathogenesis. Lancet Neurol. 2004;3:291–304.
135. Lebranchu P, Le Meur G, Magot A, David A, Verny C, Weber M, et al. Maculopathy and spinocerebellar ataxia type 1: a new association? J Neuroophthalmol. 2013;33:225–31.
136. Vaclavik V, Borruat FX, Ambresin A, Munier FL. Novel maculopathy in patients with spinocerebellar ataxia type 1 autofluorescence findings and functional characteristics. JAMA Ophthalmol. 2013;131:536–8.
137. Abe T, Abe K, Tsuda T, Itoyama Y, Tamai M. Ophthalmological findings in patients with spinocerebellar ataxia type 1 are not correlated with neurological anticipation. Graefes Arch Clin Exp Ophthalmol. 2001;239:722–8.
138. Abe T, Abe K, Aoki M, Itoyama Y, Tamai M. Ocular changes in patients with spinocerebellar degeneration and repeated trinucleotide expansion of spinocerebellar ataxia type 1 gene. Arch Ophthalmol. 1997;115:231–6.

139. Abele M, Bürk K, Andres F, Topka H, Laccone F, Bösch S, et al. Autosomal dominant cerebellar ataxia type I. Nerve conduction and evoked potential studies in families with SCA1, SCA2 and SCA3. Brain. 1997;120:2141–8.
140. Perretti A, Santoro L, Lanzillo B, Filla A, De Michele G, Barbieri F, et al. Autosomal dominant cerebellar ataxia type I: multimodal electrophysiological study and comparison between SCA1 and SCA2 patients. J Neurol Sci. 1996;142:45–53.
141. Robitaille Y, Schut L, Kish SJ. Structural and immunocytochemical features of olivopontocerebellar atrophy caused by the spinocerebellar ataxia type 1 (SCA-1) mutation define a unique phenotype. Acta Neuropathol. 1995;90:572–81.
142. Stricker S, Oberwahrenbrock T, Zimmermann H, Schroeter J, Endres M, Brandt AU, et al. Temporal retinal nerve fiber loss in patients with spinocerebellar ataxia type 1. PLoS One. 2011;6:e23024.
143. Varsányi B, Somfai GM, Lesch B, Vámos R, Farkas A, et al. Optical coherence tomography of the macula in congenital achromatopsia. Invest Ophthalmol Vis Sci. 2007;48:2249–53.
144. Birch DG, Wen Y, Locke K, Hood DC. Rod sensitivity, cone sensitivity, and photoreceptor layer thickness in retinal degenerative diseases. Invest Ophthalmol Vis Sci. 2011;52:7141–7.
145. Aleman TS, Cideciyan AV, Volpe NJ, Stevanin G, Brice A, Jacobson SG. Spinocerebellar ataxia type 7 (SCA7) shows a cone-rod dystrophy phenotype. Exp Eye Res. 2002;74:737e45.
146. Gouw LG, Digre KB, Harris CP, Haines JH, Ptacek LJ. Autosomal dominant cerebellar ataxia with retinal degeneration: clinical, neuropathologic, and genetic analysis of a large kindred. Neurology. 1994;44:1441–7.
147. Cancel G, Duyckaerts C, Holmberg M, Zander C, Yvert G, Lebre AS, et al. Distribution of ataxin-7 in normal human brain and retina. Brain. 2000;123:2519–30.
148. La Spada AR, Fu Y, Sopher BL, Libby RT, Wang X, Li LY, et al. Polyglutamine-expanded ataxin-7 antagonizes CRX function and induces cone-rod dystrophy in a mouse model of SCA7. Neuron. 2001;31:913–27.
149. Kumar N, Pulido JS. High-definition spectral domain optical coherence tomography in the evaluation of ataxia with visual impairment. Br J Ophthalmol. 2011;95:591–8.
150. Manrique RK, Noval S, Aguilar-Amat MJ, Arpa J, Rosa I, Contreras I. Ophthalmic features of spinocerebellar ataxia type 7. J Neuroophthalmol. 2009;29:174–9.
151. Ahn JK, Seo JM, Chung H, Yu HG. Anatomical and functional characteristics in atrophic maculopathy associated with spinocerebellar ataxia type 7. Am J Ophthalmol. 2005;139:923–5.
152. McLaughlin ME. Dryja TP ocular findings in spinocerebellar ataxia 7. Arch Ophthalmol. 2002;120:655–9.
153. Levinson JD, Yan J, Lambert SR, Shankar SP. Multimodal imaging of a family with spinocerebellar ataxia type 7 demonstrating phenotypic variation and progression of retinal degeneration. Retin Cases Brief Rep. 2016;10(3):267–72.
154. Teive HAG, Munhoz RP, Arruda WO, et al. Spinocerebellar ataxia type 10 - a review. Parkinsonism Relat Disord. 2011;17:655–61.
155. Spina Tensini F, Sato MT, Shiokawa N, Ashizawa T, Teive HAG. A comparative optical coherence tomography study of spinocerebellar ataxia types 3 and 10. Cerebellum. 2017;16(4):797–801.
156. Gowrisankaran S, Anastasakis A, Fishman GA, Alexander KR. Structural and Functional Measures of Inner Retinal Integrity Following Visual Acuity Improvement in a Patient with Hereditary Motor and Sensory Neuropathy Type VI. Ophthalmic Genetics 2011;32 (3):188–92.
157. Grainger BT, Papchenko TL, Danesh-Meyer HV. Optic nerve atrophy in adrenoleukodystrophy detectable by optic coherence tomography. J Clini Neurosci. 2010;17(1):122–4.